

Photoluminescence study of interfaces between heavily doped Al 0.48 In 0.52 As:Si layers and InP (Fe) substrates

L. C. Poças, J. L. Duarte, I. F. L. Dias, E. Laureto, S. A. Lourenço, D. O. Toginho Filho, E. A. Meneses, I. Mazzaro, and J. C. Harmand

Citation: [Journal of Applied Physics](#) **91**, 8999 (2002); doi: 10.1063/1.1475370

View online: <http://dx.doi.org/10.1063/1.1475370>

View Table of Contents: <http://scitation.aip.org/content/aip/journal/jap/91/11?ver=pdfcov>

Published by the [AIP Publishing](#)

Articles you may be interested in

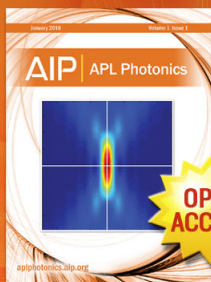
[Molecular beam epitaxial growth of AlGaPSb and AlGaPSb/InP distributed Bragg reflectors on InP](#)
J. Vac. Sci. Technol. B **22**, 1468 (2004); 10.1116/1.1669600

[High-quality InAlAs layers grown on \(411\)A-oriented InP substrates by molecular beam epitaxy](#)
J. Vac. Sci. Technol. B **17**, 1482 (1999); 10.1116/1.590778

[Investigation of optical properties of interfaces between heavily doped Al 0.48 In 0.52 As:Si and InP \(Fe\) substrates by photoreflectance analysis](#)
J. Appl. Phys. **85**, 4184 (1999); 10.1063/1.370329

[Photoluminescence study of the interface in type II InAlAs-InP heterostructures](#)
J. Appl. Phys. **84**, 2138 (1998); 10.1063/1.368275

[Deep levels in heavily Zn-doped InP layers implanted with Ti and Ti/P](#)
J. Appl. Phys. **83**, 2366 (1998); 10.1063/1.366981



Launching in 2016!
The future of applied photonics research is here

AIP | APL
Photonics

Photoluminescence study of interfaces between heavily doped $\text{Al}_{0.48}\text{In}_{0.52}\text{As}:\text{Si}$ layers and InP (Fe) substrates

L. C. Poças, J. L. Duarte,^{a)} I. F. L. Dias, E. Laureto, S. A. Lourenço,
and D. O. Toginho Filho

Departamento de Física, Centro de Ciências Exatas, Universidade Estadual de Londrina Caixa Postal 6001, CEP 86051-990, Londrina-PR, Brazil

E. A. Meneses

Instituto de Física Gleb Wataghin, IFGW-UNICAMP CEP 13083-970, Campinas, SP, Brazil

I. Mazzaro

Departamento de Física, Universidade Federal do Paraná, Caixa Postal 19091, CEP 81531-990, Curitiba-PR, Brazil

J. C. Harmand

Laboratoire Concepts et Dispositifs pour la Photonique (CNRS), 196 Avenue Henry-Ravera, 92220, Bagneux, France

(Received 4 January 2002; accepted for publication 11 March 2002)

Properties of the interface between the epitaxial layer of heavily doped $\text{Al}_{0.48}\text{In}_{0.52}\text{As}:\text{Si}$ and the $\text{InP}(\text{Fe})$ substrate are investigated by photoluminescence in $\text{AlInAs}:\text{Si}/\text{InP}(\text{Fe})$ heterostructures grown by molecular beam epitaxy. The effect on heterostructure optical properties of including a thin $\text{Al}_{0.22}\text{Ga}_{0.26}\text{In}_{0.52}\text{As}:\text{Si}$ layer at the interface is investigated as well. To explain the different interface emission energies observed, the results are analyzed by using the mixed-type I–II interface model, which considers in the type II interface a narrow InAs well, with variable width, between AlInAs and InP . The observation of the interface emission at energies as high as 1.36 eV, at low excitation intensity, is explained taking into account the high doping level of the samples. The observed interface transition luminescence thermal quenching is tentatively explained by analyzing the spatial distribution of electrons in the triangular quantum well formed at the type II interface (or at the mixed I–II interface) as a function of the temperature. © 2002 American Institute of Physics. [DOI: 10.1063/1.1475370]

I. INTRODUCTION

Materials of the $\text{Al}_x\text{Ga}_y\text{In}_{1-x-y}\text{As}$ family, grown lattice matched to InP , have been investigated and used as alternative materials, with some advantages, to the InGaAsP family for applications in microelectronics and optoelectronics devices.^{1–5} Particular importance has been given to the ternaries $\text{Al}_x\text{In}_{1-x}\text{As}$ and $\text{Ga}_y\text{In}_{1-y}\text{As}$,^{5–7} which are, respectively, the materials with the widest and the narrowest energy band gaps of that family which can be grown lattice matched to InP .

The lattice matched heterojunction $\text{Al}_{0.48}\text{In}_{0.52}\text{As}/\text{InP}$ presents a type II interface with band bending which produces a bidimensional confinement for electrons on the InP side and for holes on the AlInAs side,⁸ as shown in Fig. 1(a). This interface can be used for making new optoelectronic devices,¹ and the large conduction band offset at the interface makes this system very attractive for making high-electron-mobility transistors using the electron channel on the InP side.^{7,9,10} Radiative recombination with emission energy below the fundamental gap should be observed due to the small overlap of electron and hole wave functions. The energy of these emissions depends essentially on the conduction band discontinuity. However, preparation of type II interfaces in

AlInAs/InP structures presents many problems.^{11,12} In molecular beam epitaxy growth of AlInAs made directly on InP substrates, an As flux is usually employed in order to provide the oxide desorption of the substrate. This procedure can create a nonintentional very thin strained epilayer of InAs at the interface between the AlInAs and the InP .¹¹ As the InAs epilayer has a very narrow band gap, a quantum well would be formed at the interface, giving origin to a type I structure instead of a type II.¹¹ However, this subject is still controversial. Many experimental works have investigated the emission due to the AlInAs/InP interface but the reported results cover the large energy range from 1.1 to 1.3 eV.^{5,7,12–24} This large dispersion of results has been attributed to many factors

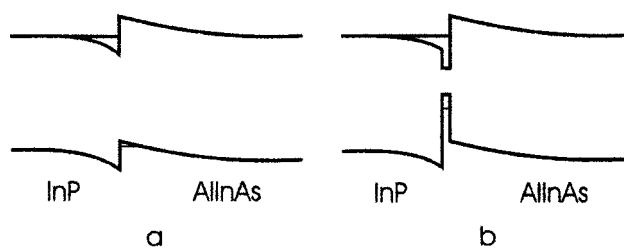


FIG. 1. Band structure diagram for: (a) pure-type II interface and (b) mixed-type I–II interface.

^{a)}Electronic mail: jlduarte@uel.br

TABLE I. Sample data, where N_D stands for the carrier concentration and $(\Delta a/a)_\perp$ is the lattice mismatch parameter.

Sample	Layer of AlGaInAs	N_D (cm ⁻³)	$(\Delta a/a)_\perp$
A	No	2.9×10^{18}	$< 0.5 \times 10^{-3}$
BQ	Yes	4.9×10^{18}	2.0×10^{-3}
C	No	6.8×10^{18}	1.7×10^{-3}
D	No	1.1×10^{19}	$< 0.5 \times 10^{-3}$

such as defects or composition gradients located at the interface^{7,14–16} and the quantum well due to the InAs layer.^{11,12}

Recently, Vignaud *et al.*²⁵ and Duez *et al.*²⁶ have proposed a model in which the interface recombination in AlInAs/InP is labeled as mixed type I–II. Figure 1 shows the diagrams for the pure type II interface [Fig. 1(a)] and the mixed type I–II interface [Fig. 1(b)], for comparison.

In the mixed type I–II recombination model, the presence of a narrow InAs well (type I structure) between InP and AlInAs is considered. In this case, the wave functions of electrons in the conduction band are spread between InP and InAs, whereas in valence band the holes are strictly confined in the InAs well.²⁶ So, the shift of the interface emission to lower energy in some samples, in comparison with the type II emission, is due to the strong decrease of the hole ground state energy that occurs when the InAs well width increases.

In the present work, the interface radiative recombination of heavily doped (10^{18} – 10^{19} cm⁻³) Al_{0.48}In_{0.52}As:Si layers grown on InP (Fe) substrate is systematically investigated by the photoluminescence (PL) technique, using a set of samples with different silicon concentrations. Also, the influence on heterostructure emission properties of a Al_{0.22}Ga_{0.26}In_{0.52}As thin layer (11 Å) grown between the InP and the AlInAs layer is investigated.

II. EXPERIMENT

The samples used in this work were 1-μm-thick Al_{0.48}In_{0.52}As:Si layers grown by molecular beam epitaxy on InP(Fe)-(001) oriented substrates. According to x-ray diffraction measurements carried out on these samples, the layers are approximately lattice matched to InP, as shown in Table I by the $(\Delta a/a)_\perp$ parameter. In sample BQ, a layer of AlGaInAs approximately 11 Å thick was grown at the interface between the InP substrate and the ternary AlInAs layer and also at the sample surface. Silicon doping levels in the ternary layers, as obtained from Hall measurements at room temperature, are also shown in Table I. Carrier concentration in the substrate is in the 10^{16} cm⁻³ range.

The samples with different silicon concentrations are identified, in increasing order of doping, by the letters A, B, C, and D. The letter Q in BQ accounts for the special case where a thin layer (11 Å) of the quaternary Al_{0.22}Ga_{0.26}In_{0.52}As was grown at the interface between the InP substrate and the AlInAs layer and also at the sample surface.

Photoluminescence (PL) measurements were performed using the 5145 Å line of a continuous wave argon ion laser

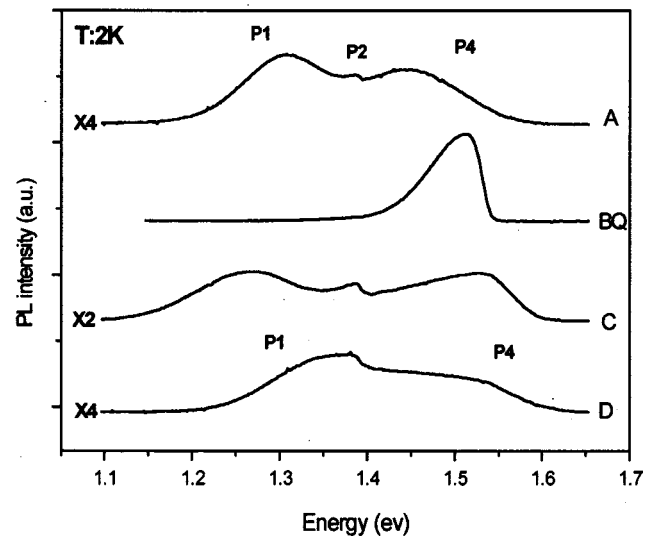


FIG. 2. Spectra of PL obtained at the temperature of 2 K for samples listed in Table I.

focused on a 300-μm-diam spot. PL signal was analyzed by a 0.5 m SPEX spectrometer coupled to a cooled Ge photo-detector. The incident power could be varied by neutral density filters and the temperature could be varied from 2 K to room temperature.

III. EXPERIMENTAL RESULTS AND DISCUSSION

A. Photoluminescence spectra

The PL spectra of the Al_{0.48}In_{0.52}As:Si/InP sample set obtained at 2 K, with an excitation beam intensity of about 14 W/cm² (10 mW power), are shown in Fig. 2.

The spectra of samples A and C are composed of two intense emission bands labeled P1 and P4, at the lowest and at the highest energies, respectively, and a third peak labeled P2 located between the other two, in the 1.385–1.387 eV region. In sample D, the three peaks merge. For sample BQ, which has the AlGaInAs layer at the interface between InP and AlInAs, only the P4 transition is observed.

The P4 emission band is associated with the AlInAs layer emission and the changes that take place in this emission when the silicon doping concentration changes can also be seen in Fig. 2. An analysis of the spectra of samples A, BQ, and C shows that the P4 peak displaces to higher energies when the doping concentration increases. This displacement is difficult to observe in sample D since the lower energy band merges with the P2 and P4 ones. However, it is possible to observe that in this sample, which has the highest doping level, the emission spreads to higher energies. In sample A, where the maximum intensity of this emission is below the known values for the Al_{0.48}In_{0.52}As energy band gap, this energy displacement is attributed to the presence of acceptor impurities in AlInAs, which makes donor–acceptor (D–A) transitions possible. This possibility was verified by PL spectra obtained at different intensities (not shown here), which has shown an energy displacement to higher values when the intensity is increased, a characteristic behavior of the (D–A) emission.

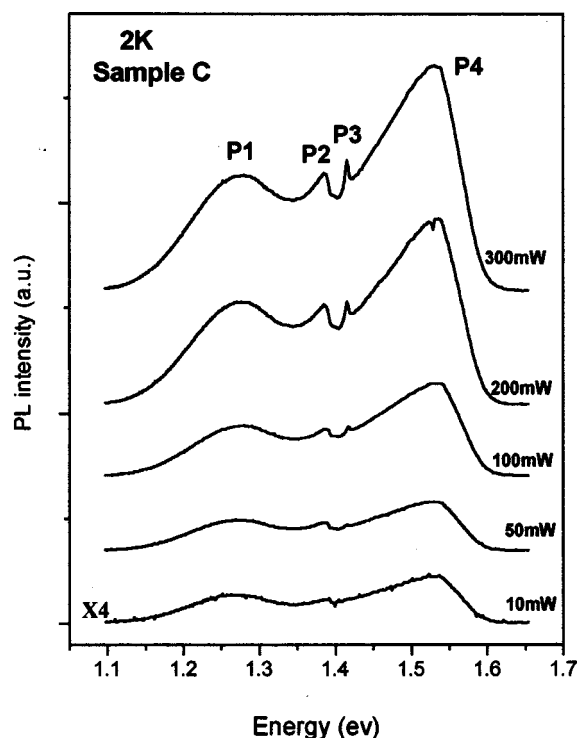


FIG. 3. Photoluminescence spectra obtained with power variation for the sample C.

The lowest energy band ($P1$), which is located at an energy lower than the InP and AlInAs energy band gaps, is related to the emission that takes place at the interface. This emission is evident in the A, C, and D sample spectra, whereas in the sample D spectrum it merges with the $P2$ and $P4$ bands. In the spectrum of sample BQ, the sample which has the quaternary AlGaInAs layer at the interface, this low energy band is completely absent.

For intensities a little higher than that used in the previously shown spectra, but also at 2 K, another peak, at 1.414 eV, appears and was labeled $P3$, as shown in Fig. 3. The $P3$ peak was identified as being due to excitons bound to the acceptor impurities of the InP substrate and the $P2$ peak was attributed to the acceptor impurities in InP substrate, whose ionization energy corresponds to that of Mg.^{27,28}

The interface emission ($P1$) behavior as a function of the incident power can be seen in Fig. 3, for sample C. When the incident power is raised from 10 to 300 mW, the energy of maximum emission shifts from 1.267 to 1.280 eV. This shift to higher energies is also observed in samples A and D, but it is difficult to follow this shift in sample D due to the strong overlap of all transitions in this sample. This shift to higher energies when the excitation intensity is raised is a characteristic of type II (or mixed type I–II) transition,^{8,26} as will be discussed later. Regarding the $P1$ emission intensity in comparison with the other emissions, when the incident power is raised, it increases a little at the beginning until it reaches a maximum and then it decreases.

Figure 4 shows sample C emission spectra from 2 to 100 K. As the temperature is raised, the interface emission intensity increases a little until it reaches a maximum (at about 20 K) and then decreases, vanishing at a temperature around 100 K. Samples A and D show similar behavior.

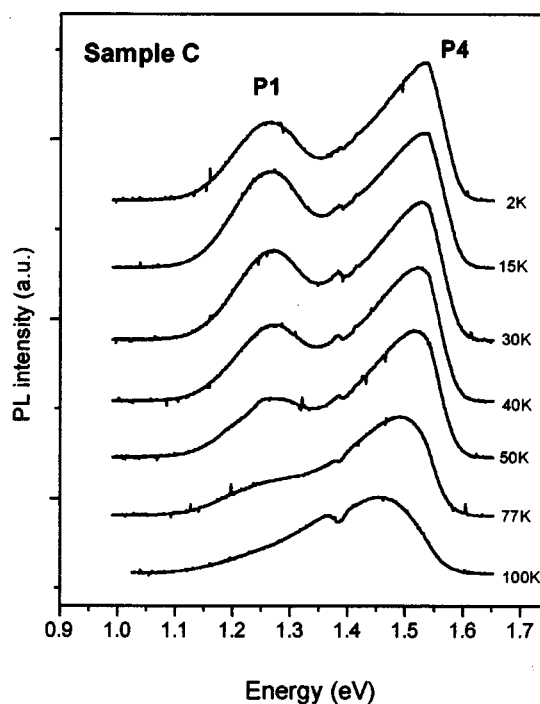


FIG. 4. PL spectra obtained with temperature variation between 2 and 100 K for the sample C.

Although this behavior of decreasing emission intensity with increasing temperature is a characteristic of transitions in which impurities are involved, there is some strong evidence that the $P1$ emission is due not to impurities but to transitions that take place at the interface. One evidence is the fact that this emission occurs at different energies for different samples, as seen in Fig. 2. According to x-ray measurements, the AlInAs layers are approximately lattice matched to InP and therefore have approximately the same energy band gap in all the samples. The displacements of the $P4$ emission band, from one sample to another, are due to shallow impurities (the Si dopant as well as other nonintentional shallow impurities). So, if the $P1$ emission was due to any deep impurity, in AlInAs or in InP, it should be at the same position, at least roughly, in all samples. Moreover, if $P1$ was due to a deep impurity, it should not disappear at a relatively low temperature.

Another very strong evidence that the $P1$ emission is not due to impurities is the fact that in sample BQ, in which the quaternary AlGaInAs was grown between AlInAs and InP, this emission is not observed, even at a high excitation power. On the other hand, this is evidence that this emission originates at the interface between AlInAs and InP.

Thus, experimental evidence has shown clearly that the $P1$ emission originates at the AlInAs/InP interface.

Figure 4 also shows the $P1$ emission peak energy shift to higher energies with the increase in temperature.

B. Discussion of the interface recombination energy

In this section, the values for the interface emission energy obtained by the present work are analyzed according to the mixed type I–II interface model and the value which is attributed to the pure type II emission is compared to the

corresponding one of Ref. 25, taking into account that in the sample used in this work the doping level is three orders of magnitude larger than that of Ref. 25.

The diversity of values found by the present work for the energy of maximum *P1* emission at low excitation intensity (1.31 eV for sample A, 1.27 eV for sample C, and ~ 1.36 eV for sample D, as can be seen in Fig. 2) and the fact that the order of energy values does not follow the order of the doping level (for example, for sample A, the emission energy is higher than that for sample C, which is less doped than A, whereas the emission energy of sample D, the most doped sample, is higher than the emission energies of samples A and C), can be explained, at least qualitatively, by the mixed type I–II interface model. According to that model, sample D ($E \sim 1.36$ eV) would not have the InAs layer, while sample A ($E = 1.31$ eV) would have an InAs layer of intermediate thickness and sample C ($E = 1.27$ eV) would have the thickest InAs layer.

The difference between the energy of the pure type II emission (for interface without the InAs layer) observed in sample D of this work and the corresponding energy reported in Ref. 25 (1.27–1.28 eV), both for low intensity excitation, can be accounted for the difference in the doping level between the samples ($1.1 \times 10^{-19} \text{ cm}^{-3}$ for sample D and $\sim 10^{16} \text{ cm}^{-3}$ for sample of Ref. 25). To better understand this process, it is interesting to analyze the behavior of the electron ground state energy level (E_0) and the electron distribution in the triangular quantum well for electrons (EW) in the conduction band, at the InP side of the interface (see Fig. 5), as a function of the Si concentration in AlInAs. As donor concentration (Si) in AlInAs increases, the Fermi level is raised and the electrons are transferred from the AlInAs to the InP side in order to equalize the Fermi level on both sides.²⁹ This electron transfer fills the EW level, raising the Fermi level on the InP side and it also raises the electrostatic potential in the region close to the interface, as the number of ionized Si at the AlInAs side also increases. As the electron density in EW increases, the E_0 ground state of this well also increases^{8,29} and, as a consequence of the overall process, the energy of the interface emission shifts to higher energies.

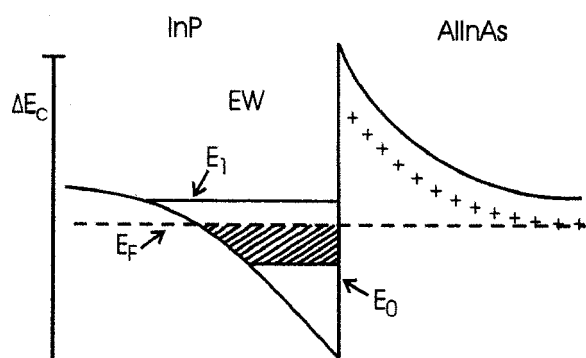


FIG. 5. Conduction band diagram at the InP/AlInAs interface representing the electron filling of the EW triangular well due to the AlInAs doping. E_0 and E_1 denote the lowest EW levels, E_F refers to the Fermi level and ΔE_C refers to the conduction band discontinuity.

The assumption that the difference between the value for the type II emission energy in the slightly doped sample of Ref. 25 ($E \sim 1.28$ eV) and the corresponding value for the heavily doped sample found by the present work ($E \sim 1.36$ eV) is due to the difference in the doping level is reinforced by the fact that Ref. 25 reports a strong dependence of type II transition energy (E) on the excitation intensity (the minimum $E = 1.27$ – 1.28 eV at the low intensity limit and the maximum $E \sim 1.36$ eV at a very high intensity, $\sim 60 \times 10^3 \text{ W/cm}^2$), where the maximum E value is approximately the same value that was measured by the present work using low excitation intensity. This can be explained by the fact that an increase in the excitation intensity results in an increase in the densities of photogenerated electrons in EW and of photogenerated holes in the valence band well (HW) on the AlInAs side. The photogenerated electrons raise the EW ground state and the photogenerated holes raise the HW ground state and, as a consequence, the interface emission is shifted to higher energies.^{8,26} So, this shift only takes place because the incident light creates positive and negative charges on different sides of the interface, as in the doping case.

C. Analysis of the emission intensity dependence on temperature

In this section, the behavior of the *P1* interface emission intensity with temperature is analyzed. In general, all samples show the following behavior: the emission intensity increases slightly whenever the temperature rises from 0 to 15–20 K and then decreases, vanishing at temperatures between 70 and 100 K. To better estimate this change, the *P1* emission integrated intensity was evaluated for each temperature used and, with these results, a plot of the integrated intensity (I) as a function of the inverse of the temperature was made and the experimental points were fitted by the expression (Arrhenius plot)

$$I = \frac{I_0}{1 + C_1 \exp(-E_a/K_B T)}, \quad (1)$$

where C_1 and E_a are parameters to be evaluated by this fit. Due to the behavior in which the emission intensity increases slightly before decreasing and in order to have a good fit for expression (1), inferring thereby the activation energy E_a , the experimental point obtained at 2 K temperature was not taken into account. This procedure was repeated for all samples. Figure 6 shows the best fit of expression (1) (continuous line) with the experimental points.

The C_1 and E_a (activation energy) parameters obtained for each sample are shown in Table II; the values for sample D are highly uncertain due to the fact that the *P1*, *P2*, and *P4* emission curves overlap, making the evaluation of the *P1* integrated intensity difficult.

Table II shows all samples with a low activation energy between 10 and 20 meV.

Next, an explanation for the fact that the *P1* emission intensity decreases with the increase in temperature is suggested, based on the analysis of the triangular well for electrons (EW) in the conduction band on the InP side and the

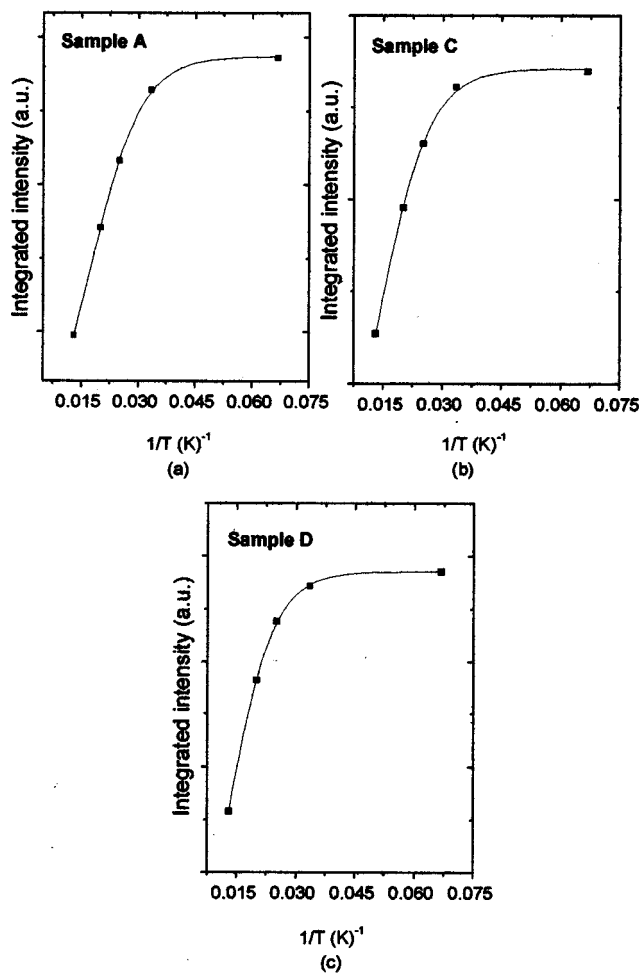


FIG. 6. Plot of the integrated intensity for the interface emission vs the inverse of the temperature (dots) and the corresponding best fit (continuous line), for: (a) sample A, (b) sample C, and (c) sample D.

triangular well for holes (HW) in the valence band on the AlInAs side, as seen in Fig. 1(a) for a type II interface. Considering that, in order to have a type II emission at the interface, a spatial overlap of the electron (in EW) and hole (in HW) wave functions is necessary, the behavior as a function of the temperature of the wave function spatial distribution for electrons and holes and its action on the interface emission efficiency are analyzed. The analysis of electrons in a type II interface will be done initially and, then, the discussion will be extended to the electrons and holes in the type II and mixed type I–II interfaces.

The electrons confined in EW are subjected, at the AlInAs side, to a sharp potential barrier of approximately 250 meV and, at the InP side, to a triangular potential barrier

much smaller and with a much smaller slope. So, as the temperature is raised, the electrons in EW are thermally excited to higher energy states, resulting in a spread of the wave functions to regions further from the interface (see Fig. 5). Then, the electron wave function penetration in the barrier created by AlInAs layer decreases and, as a consequence, the spatial overlap of the electron and hole wave functions decreases, thereby decreasing the probability of a spatially indirect recombination occurring across the interface. In addition, as the temperature increases and the electrons are excited to higher energy states, they are constrained by a lower triangular barrier at the InP side (at the AlInAs side this change is negligible, due to the large difference in height of both barriers), which makes the wave function penetrate more in the InP barrier and less in the AlInAs, decreasing the indirect radiative emission. An argument similar to this one was recently used to explain the luminescence thermal quenching in a *p*-type δ -doping structure.^{30,31} For even higher temperatures, the electrons are excited to nonlocalized states and the wave function penetration in AlInAs is further reduced.

An analogous process should occur with the holes in HW, in the valence band, for a type II transition. When the interface is mixed type I–II, the hole should be confined by the InAs well, as previously described, and thereby only electrons will contribute to the quenching process.

IV. CONCLUSIONS

From the low temperature photoluminescence spectra, it was possible to identify the emission due to the AlInAs:Si epitaxial layer and that due to the InP(Fe) substrate. An emission at a lower energy, identified as being due to a transition which takes place at the interface, whose energy varies significantly from one sample to the other and which is absent in the sample that has the AlGaInAs thin layer at the interface, was also observed. Using the mixed-type I–II interface model, which considers a type II interface combined with a narrow InAs well between the AlInAs and InP, it is possible to explain qualitatively the different emission energies for different samples by considering InAs wells with different thickness. The observation of the maximum interface emission at an energy as high as 1.36 eV, at low excitation intensity, can be accounted for by the high doping level of the sample. In addition, the luminescence thermal quenching observed in this work can be understood by analyzing the spatial distribution of electrons in the triangular quantum well formed at the type II interface (or at the mixed type I–II interface) as a function of temperature.

ACKNOWLEDGMENTS

This work was partially supported by the Brazilian Agencies FBB, CAPES, and CNPq.

TABLE II. Parameters E_a (activation energy) and C_1 obtained by fitting experimental values of P_1 integrated intensity with the expression $I = I_0 / [1 + C_1 \exp(-E_a/K_B T)]$.

Sample	E_a (meV)	C_1
A	13 ± 2	14
C	13 ± 2	9
D	15 ± 5	8

¹M. Sacilotti, F. Motisuke, Y. Monteil, P. Abraham, F. Iikawa, C. Montes, M. Furtado, L. Horiuchi, R. Landers, J. Morais, L. Cardoso, J. Decobert, and B. Waldman, *J. Cryst. Growth* **124**, 589 (1992).

²M. Quillec, *Proc. SPIE* **1361**, 34 (1991).

³E. Laureto, I. F. L. Dias, J. L. Duarte, E. Di Mauro, H. Iwamoto, M. T. P.

- Freitas, S. A. Lourenço, D. O. Toginho Filho, and J. C. Harmand, *J. Appl. Phys.* **85**, 1 (1999).
- ⁴M. J. Mondry, D. I. Babic, J. E. Bowers, and L. A. Coldren, *IEEE Photonics Technol. Lett.* **4**, 627 (1992).
- ⁵R. Bhat, M. Koza, K. Kash, S. Allen, W. Hong, S. Schwartz, G. Chang, and P. Lin, *J. Cryst. Growth* **108**, 441 (1991).
- ⁶F. Capasso, C. Gmachl, R. Paiella, A. Tredicucci, A. L. Hutchinson, D. L. Sivco, J. N. Baillargeon, A. Y. Cho, and H. C. Liu, *IEEE J. Sel. Top. Quantum Electron.* **6**, 931 (2000).
- ⁷P. Abraham, M. A. Garcia Perez, T. Benyattou, G. Guillot, M. Sacilotti, and X. Letartre, *Semicond. Sci. Technol.* **10**, 1585 (1995).
- ⁸H. Kroemer and G. Griffiths, *IEEE Electron Device Lett.* **4**, 20 (1983).
- ⁹M. A. Fathimulla, T. Loughran, L. Stecker, E. Hempfling, M. Mattingly, and L. Aina, *IEEE Electron Device Lett.* **EDL-9**, 223 (1988).
- ¹⁰C. M. Hanson, P. Chu, H. H. Wieder, and A. R. Clawson, *IEEE Electron Device Lett.* **EDL-8**, 52 (1987).
- ¹¹D. Vignaud, X. Wallart, and F. Mollot, *J. Appl. Phys.* **76**, 2324 (1994).
- ¹²M. J. S. P. Brasil, R. E. Nahory, W. E. Quinn, M. C. Tamargo, and H. H. Farrell, *Appl. Phys. Lett.* **60**, 1981 (1992).
- ¹³L. Aina, M. Mattingly, and L. Stecker, *Appl. Phys. Lett.* **53**, 1620 (1988).
- ¹⁴E. Lugagne-Delpon, J. P. André, and P. Voisin, *Solid State Commun.* **86**, 1 (1993).
- ¹⁵P. Abraham, Y. Monteil, M. Sacilotti, T. Benyattou, M. A. Garcia, S. Moneger, A. Tabata, R. Landers, J. Morais, and M. Pitaval, *Appl. Surf. Sci.* **65/66**, 777 (1993).
- ¹⁶J. Böher, A. Krost, R. Heitz, F. Heinrichsdorff, L. Eckey, D. Bimberg, and H. Cerva, *Appl. Phys. Lett.* **68**, 1072 (1996).
- ¹⁷S. M. Olsthoorn, F. A. J. M. Diressen, and L. J. Giling, *J. Appl. Phys.* **73**, 7804 (1993).
- ¹⁸J. Böher, A. Krost, and D. Bimberg, *J. Vac. Sci. Technol. B* **11**, 1642 (1993).
- ¹⁹N. Pan, J. Carter, J. Elliot, H. Hendriks, S. Brierley, and K. C. Hsieh, *Appl. Phys. Lett.* **63**, 3029 (1993).
- ²⁰R. Sakamoto, T. Kohno, T. Kaniyoshi, M. Inoue, S. Nakajima, and H. Hayashi, *Semicond. Sci. Technol.* **7**, 271 (1992).
- ²¹A. Titkov, W. Seidel, J. P. André, P. Voisin, and M. Voos, *Solid-State Electron.* **37**, 1041 (1994).
- ²²D. Bimberg, J. Böher, and A. Krost, *J. Vac. Sci. Technol. A* **12**, 1039 (1994).
- ²³Y. Kawamura, A. Kamada, K. Yoshimatsu, H. Kobayashi, H. Iwamura, and N. Inoue, *Inst. Phys. Conf. Ser.* **155**, 129 (1997).
- ²⁴K. Borgi, M. Hjiri, F. Hassen, H. Maaref, V. Souliere, and Y. Monteil, *Microelectron. Eng.* **51**, 299 (2000).
- ²⁵D. Vignaud, X. Wallart, F. Mollot, and B. Sermage, *J. Appl. Phys.* **84**, 2138 (1998).
- ²⁶V. Duez, O. Vanbésien, D. Lippens, D. Vignaud, X. Wallart, and F. Mollot, *J. Appl. Phys.* **85**, 2202 (1999).
- ²⁷F. R. Bacher, in *Properties of Indium Phosphide*, Emis Datareviews Series 6 (INSPEC, London, 1991), p. 205.
- ²⁸A. A. Iliadis and S. Ovadia, *J. Appl. Phys.* **63**, 5460 (1988).
- ²⁹C. Weisbuch, *Semiconductors and Semimetals, Applications of Multiquantum Wells, Selective Doping, and Superlattices*, (edited by E. Dingle, Academic Press, San Diego, 1987), Vol. 24, p. 30.
- ³⁰G. M. Sipahi, R. Enderlein, L. M. R. Scolfaro, J. R. Leite, E. C. F. da Silva, and A. Levigne, *Phys. Rev. B* **57**, 9168 (1998).
- ³¹A. Levigne, E. C. F. da Silva, G. M. Sipahi, A. A. Quivy, L. M. R. Scolfaro, J. R. Leite, I. F. L. Dias, E. Laureto, J. B. B. de Oliveira, E. A. Menezes, and A. G. Oliveira, *Phys. Rev. B* **59**, 4634 (1999).